Conceptual approach to investigating the impact of climate change scenarios on groundwater recharge, nitrogen leaching and maize yield predictions at Wagna test site, Austria

G. Klammler, J. Fank and H. Kupfersberger

Modellansatz zur Bewertung des Einflusses von Klimawandelszenarien auf Grundwasserneubildung, Stickstoffauswaschung und Maiserträge am Versuchsfeld Wagna, Österreich

1 Introduction

The quantity and quality of groundwater depends on a wide range of factors. Especially the application of nitrogen fertilizer in agricultural areas can lead to a significant threat for shallow aquifers. E.g., the Murtal aquifer south of Graz, Austria, is used at a 76 % for agriculture, but also supplies drinking water up to 1.500 L/s. In order to guarantee regional drinking water supply and to protect groundwater dependent ecosystems, groundwater resources must be managed in a sustainable way. I.e., groundwater quantity should be safeguarded in the long term and groundwater quality should comply with the Groundwater Directive (GWD, 2006). A further and equally important task is the agricultural crop production, which is indispensable for an autonomic and regional food supply as well as for the socioeconomic existence of farmers. However, since intensive agriculture can be a source of diffuse nitrogen input into the groundwater, the coexistence of drinking water supply and agricultural crop production has to be appropriately managed in order to guarantee a sustainable dual use of these two resources.

Zusammenfassung

Quartäre Porengrundwasserleiter in Österreich beinhalten einerseits wichtige Trinkwasserressourcen, werden jedoch andererseits auch intensiv landwirtschaftlich genutzt. Diese Doppelfunktion bringt einen Nutzungskonflikt mit sich, der zum Teil stark durch diffuse Stickstoffeinträge geprägt ist und für eine nachhaltige Koexistenz harmonisiert werden muss. Daher wird der Einfluss von zukünftigen Klimaszenarien auf das Grundwasser sowie auf Maiserträge für den Standort des landwirtschaftlichen Versuchsfelds Wagna, Österreich, untersucht. Simulationen mit Hilfe eines Bodenwasserhaushalts- und Stickstofftransportmodells prognostizieren einen ansteigenden Trend von Grundwasserneubildung, Stickstoffauswaschung und Nitratkonzentrationen im Sickerwasser. Die Simulationsergebnisse der Maiserträge zeigen eine stärkere Abhängigkeit vom Niederschlag als von der Temperatur an diesem Standort. Aus diesem Grund werden keine signifikanten Ertragszuwächse ohne zusätzliche Bewässerung für das Versuchsfeld Wagna prognostiziert.

Schlagworte: Nitrat, Bodenwasserhaushaltsmodell, Stickstofftransport, Simulation.

Summary

Austria s alpine foothill aquifers contain important groundwater resources, but are also used intensively by agriculture. To safeguard regional food production and drinking water supply, this dual use has to be harmonized for a sustainable long-term coexistence. For this purpose, we investigate the influence of future climate projections on groundwater and agricultural yields at the test site Wagna in Austria. Vadose zone model simulations based on four climate change scenarios indicate an increasing trend of groundwater recharge, nitrogen leaching and nitrate concentrations in the seepage water. Maize yields are found to be more sensitive to precipitation than to temperature increase at this location. Thus, no significant maize yield increase is predicted without irrigation in the future.

Key words: Nitrate, vadose zone model, crop production, vegetation period, simulation.

According to NEUMEISTER (2010), simulation models provide state-of-the-art methods to simulate and understand complex systems in natural sciences. As a consequence, environmental, economic and political decisions for safeguarding future coexistence between agriculture and drinking water supply are commonly based on tools like saturated and unsaturated water flux and transport models. The latter ones describe hydrological processes in the vadose zone including those due to soil and plant properties under different weather conditions. This provides results for quantity and quality of unsaturated water fluxes reaching the groundwater table. Using climate change scenarios as an input for these simulation models allows quantifying the impact of future climate scenarios on groundwater and agricultural crop production.

In literature, various applications concerning effects of climate change on groundwater and/or crop yields can be found for different investigation areas. First of all, an ensemble modeling approach for climate simulations (i.e., using several climate change scenarios generated by various global circulation models) is frequently recommended, as it covers the space of global circulation model (GCM) uncertainties (GRAUX et al., 2012; SURFLEET et al., 2012; JACKSON et al., 2010; FADER et al., 2009; GODERNIAUX et al., 2009; KANG et al., 2009; SERRAT-CAPDEVILA et al., 2007; WOLDEAMLAK et al., 2007; MERRITT et al., 2006; ECKHARDT & ULBRICH, 2003; CUCULEANU et al., 2002). KANG et al. (2009) also provide a comprehensive review of literature related to the assessment of climate change impacts on crop productivity using climate, water and crop yield models. This review shows that – depending on the latitude – crop yields may increase or decrease due to changing climate. It is also mentioned that crop yields are more sensitive to precipitation than to temperature. KANG et al. (2009) generally conclude that with increasing temperature and fluctuating precipitation the water availability and crop production will decrease in the future, but if the irrigated areas are expanded, the total crop yield will increase.

For groundwater hydrological modeling it has to be considered that the land use in general, but also types and phenologies of cultivated crops, may change in the future due to different climate conditions. This change of cultivated crops in combination with different temperature and precipitation patterns affect the water and nutrient behavior in the soil. In order to consider the full complexity of interactions between the system elements climate, vegetation, soil, unsaturated and saturated groundwater, a physically based numerical solution is used in this research.

The objective of the present paper is to quantify the influence of four different climate change scenarios on groundwater recharge, nitrogen leaching and crop yields for grain maize until the year 2100. For this purpose, the numerical simulation model SIMWASER/STOTRASIM is applied after thorough calibration to lysimeter measurements at the Wagna test site, Austria. Since SIMWASER/STOTRASIM has been already successfully applied for sub-regions of the Murtal aquifer (KLAMMLER et al., 2013), this model seems suitable also for the present work. To avoid uncertainties due to upscaling, this work only focuses on the location of the lysimeter. However, soil conditions are representative for most parts of the Murtal aquifer and the conceptual basis presented should be useful for further regional modeling applications.

2 Material and Methods

2.1 Vadose Zone Model SIMWASER/STOTRASIM

SIMWASER (STENITZER, 1988) describes the one-dimensional, vertical water flux within an unsaturated soil profile. Water balance and plant growth are interrelated to the physiological interaction between transpiration and assimilation of crops. Plant growth (neglecting pests and disease) is only possible if the water supply towards the stomata meets the transpiration loss. Transpiration is deduced from evapotranspiration, which is calculated according to a modified Penman-Monteith approach (THOM & OLIVER, 1977; SZEICZ et al., 1969). Actual transpiration is limited by the amount of water which can be withdrawn from the soil by roots. In turn, actual rooting depths depend on the simulated crop as well as on the penetration resistance of the soil. Water flux between different soil layers is calculated according to the Darcy-Buckingham approach as a function of capillary conductivity and hydraulic head.

STOTRASIM (FEICHTINGER, 1998) calculates nitrogen dynamics of agriculturally used soils on a daily base. The focus is set on nitrogen leaching into groundwater, which is coupled to water fluxes simulated with SIMWASER. Subsequently, further components of the nitrogen cycle are included within STOTRASIM: N input (NO_3-N, NH_4-N and organic N out of farm and mineral fertilizer, N deposition, N in irrigation water, legumes, crop residues, capillary rise from groundwater), N turnover (mineralization, nitrification, immobilization), N transport in the soil and N export (denitrification, crop uptake, crop removal). In case of water or nitrogen shortness the plant growth is restricted; shortness of other nutrients does not affect crop yields.

The coupled simulation model SIMWASER/STOTRASIM is calibrated against seepage water, NO_3-N leaching and crop yields by means of lysimeter measurements at Wagna test site, Austria. The calibration considers the period of 2006–2011, where mainly grain maize, but also oil pumpkin and winter grain (winter barley and triticale) were cultivated. As can be seen in Figure 1, measured groundwater recharge rates are simulated with high agreement, both for annual balances and for short-term fluctuations. Modeling nitrogen leaching proves to be more difficult due to rather complex nitrogen transformation processes in the soil. Nevertheless, default plant parameters are adjusted at the lysimeter scale and the calibration results for NO_3-N leaching appear acceptable. Calibration results for total dry matter above ground are presented in Figure 2. Crop yields can be derived out of simulated dry matter by means of harvest indices (ratios of crop yield to aboveground dry matter), which are also measured at the test site.

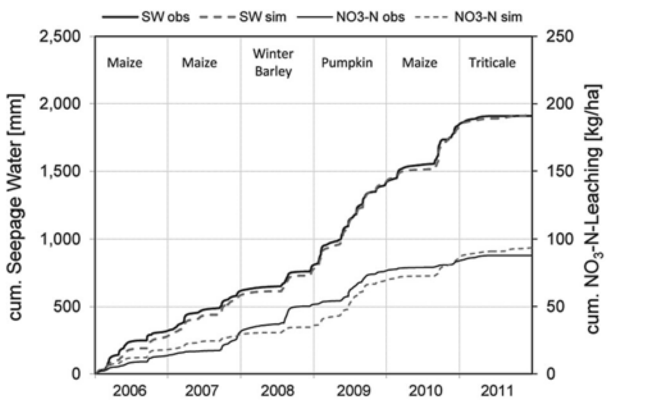

Figure 1: Comparison between observed and simulated cumulative seepage water and nitrogen leaching for the calibration period 2006–2011

Abbildung 1: Vergleich zwischen gemessenem (SW obs) und simuliertem (SW sim) kumulativen Sickerwasser sowie gemessener (NO_3 N obs) und simulierter (NO_3 N sim) kumulativer Stickstoffauswaschung für die Kalibrationsperiode 2006–2011

2.2 Climate Change Scenarios

The climate change projections used in this paper cover the period from 1961 to 2100 and are based on the *SRES A1B* (Special Report on Emissions Scenarios A1B) greenhouse gas emission scenario (NAKIĆENOVIĆ & SWART, 2000). This is an intermediate emission scenario based on the IPCC fourth assessment report (IPCC, 2007) predicting an air temperature increase of approximately 3 °C from now until

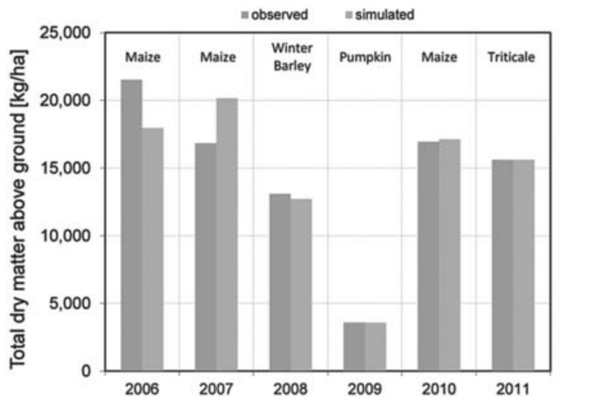

Figure 2: Comparison between observed and simulated total aboveground dry matter of main crops cultivated within the calibration period 2006–2011

Abbildung 2: Vergleich zwischen gemessener (observed) und simulierter (simulated) oberirdischer Trockenmasse für die Hauptkulturen in der Kalibrationsperiode 2006–2011

2100. The uncertainty inherent in all climate change projections is addressed by using an ensemble of scenarios produced by the four different GCMs *ECHAM5-r3* (European Centre for Medium-Term Weather Forecast Hamburg; ROECKNER et al., 2006), *IPSL* (Institute Pierre-Simon Laplace Paris), *CNRM* (National Centre of Meteorological Research France; VOLDOIRE et al., 2011; SALAS-MÉLIA et al., 2005) and *HADCM3-Q0* (Hadley Centre Coupled Model; GORDON et al., 2000). All global climate scenarios are dynamically downscaled using the Rossby Centre Regional Atmospheric model *RCA3.0* (SAMUELSSON et al., 2011; KJELLSTRÖM et al., 2005) and are provided by the Swedish Meteorological and Hydrological Institute (*SMHI*) for the required weather elements temperature, precipitation, relative humidity, wind speed and solar radiation. In addition, temperature and precipitation are also statistically downscaled by the quantile mapping approach using meteorological data from Wagna (YANG et al., 2010a and 2010b), which produces plausible results for the observed period from 1961 to 2011 (Figures 3 and 4).

Relative humidity, wind speed and solar radiation are not statistically downscaled, but are taken from the *RCA3.0* outputs (dynamical downscaling) which deviate from observed data in general. This fact is illustrated for the example of simulated wind speed in Figure 5. There it can be seen that the level of the dynamically downscaled wind speed out of all GCMs used is more than two times higher than observed. Only shifting daily wind speeds by a constant would lead to seasonal differences as presented in Figure 5b. The dynamically downscaled wind speed of GCM 2 results in

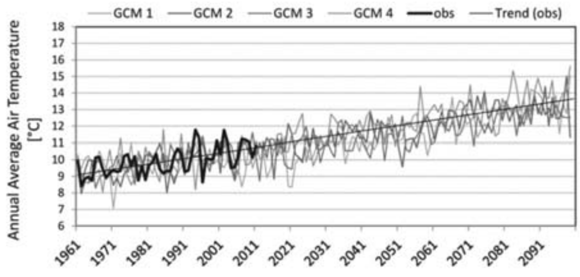

Figure 3: Observed (obs) and simulated (GCMs 1–4) annual average air temperature for Wagna, Austria, from 1961 to 2100
Abbildung 3: Gemessene (obs) und simulierte (GCMs 1–4) mittlere Jahrestemperatur für Wagna, Österreich, 1961–2100

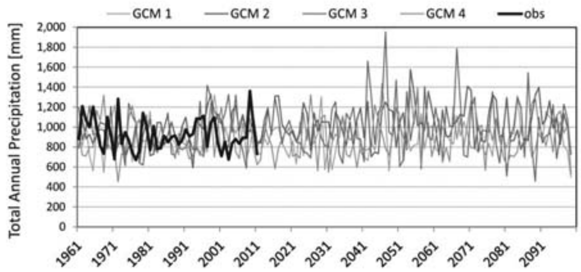

Figure 4: Observed (obs) and simulated (GCMs 1–4) total annual precipitation for Wagna, Austria, from 1961 to 2100
Abbildung 4: Gemessener (obs) und simulierter (GCMs 1–4) Jahresniederschlag für Wagna, Österreich, 1961–2100

much higher mean values in winter (November to March) than in the vegetation period (April to October). In contrast, observed wind speed shows only low seasonal differences. Thus, the datasets for wind speed, relative humidity and solar radiation were shifted separately for the summer and winter periods (Figure 5c).

These modifications in wind, humidity and radiation data are validated by means of the grass reference evapotranspiration ET_0 (ALLEN et al., 1998), which is dependent on temperature, wind speed, relative humidity and solar radiation. Figure 6 shows the cumulative ET_0 for the four climate change scenarios compared to ET_0 based on observed weather data from 1961 to 2011. Figure 6a uses the original *RCA3.0* output (dynamically, but not statistically downscaled) and Figure 6b the modified datasets for wind, humidity and radiation.

2.3 Soil conditions

To avoid uncertainties coming from soil input data, results presented in this paper are all based on simulations using one

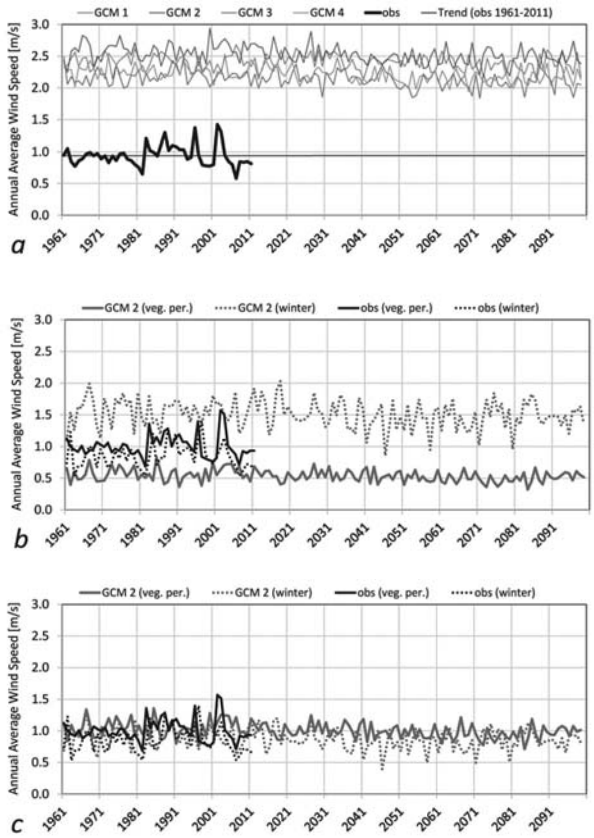

Figure 5: (a) Observed (obs) and simulated (GCMs 1–4) annual average wind speed for Wagna, Austria, from 1961 to 2100 and (b, c) procedure of data modification for not statistically downscaled weather elements
Abbildung 5: (a) Gemessene (obs) und simulierte (GCMs 1–4) mittlere jährliche Windgeschwindigkeit für Wagna, Österreich, 1961–2100 und (b, c) Prozedur der Datenmodifikation für nicht statistisch downgescalte Wetterelemente

well analyzed soil profile. This soil profile is given in Table 1 and corresponds to the lysimeter installed at the agricultural test site Wagna, Austria. In situ pF curves are also available at depth of 35, 60, 90 and 180 cm at this location.

Table 1: Soil horizons and soil textures for the simulated location
Tabelle 1: Bodenhorizonte und -texturen für den simulierten Standort

Depth [cm]	Horizon[1]	Soil texture[1,2]	(sand/silt/clay/gravel)[1,3]
0 - 30	Ap R	Ls3	(20/33/45/2)
30 - 50	B	Ls4	(20/27/53/0)
50 - 60	B	Sl4	(14/24/62/0)
60 - 200	C	Ss	(0/2/31/67)

[1]) According to AG Boden (2005)
[2]) Abbreviations account for grain size distribution < 2 mm
[3]) Classification: 0 < 0.002 < 0.063 < 2 < 63 mm

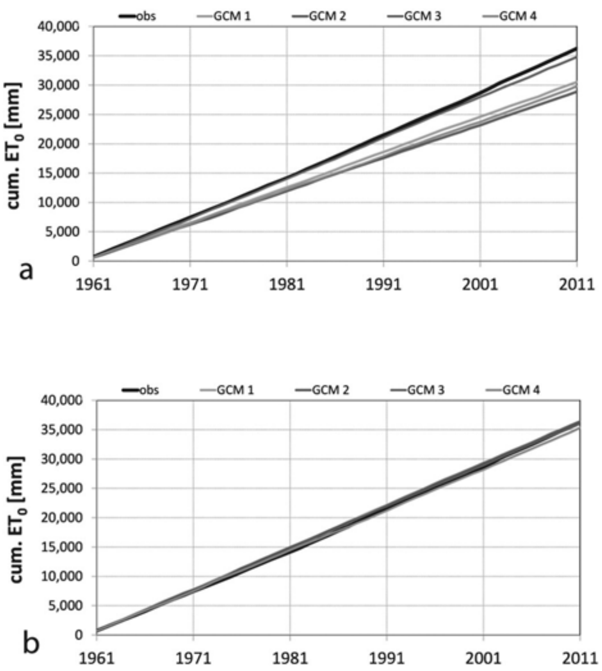

Figure 6: Grass reference evapotranspiration ET_0 for (a) uncalibrated and (b) modified wind speed, relative humidity and solar radiation

Abbildung 6: Grasreferenz-Evapotranspiration ET_0 für (a) unkalibrierte und (b) modifizierte Windgeschwindigkeit, relative Feuchte und Globalstrahlung

2.4 Vegetation

Grain maize is the most dominant crop within the Murtal aquifer between Graz and Bad Radkersburg, Austria. More than 55 % of the arable land is cultivated by grain maize, especially for pig breeding. Although SIMWASER/STOTRASIM is also calibrated for winter grain and oil pumpkin, plant development processes are most reliably described for maize. Consequently, the present work limits attention to maize production and its resulting groundwater recharge and nitrogen leaching. The following three maize cultivation strategies are simulated, which mainly differ in durations of vegetation periods and nitrogen-fertilization rates applied.

- Cultivation strategy 1 (*CS1*):
  - Date of sowing: soil temperature > 11 °C
  - Date of harvest: October 4th (in groundwater protection areas of the Murtal aquifer farmers are committed to cultivate hardy catch crops before October 10th; SGV 2005)
  - N fertilization input: 140 kg N/ha/a (according to BMLFUW, 2006)
  - Hardy catch crop: Forage rye

- Cultivation strategy 2 (*CS2*):
  - Date of sowing: soil temperature > 11 °C
  - Date of harvest: end of potential vegetation period (described in section 2.5)
  - N fertilization input: 140 kg N/ha/a (according to BMLFUW, 2006)
  - Hardy catch crop: Forage rye

- Cultivation strategy 3 (*CS3*):
  - Date of sowing: soil temperature > 11 °C
  - Date of harvest: end of potential vegetation period (described in section 2.5)
  - N fertilization input: 200 kg N/ha/a
  - No hardy catch crop

2.5 Future Vegetation Period

The potential vegetation period for grain maize mainly depends on both temperature and moisture availability (Kenny & Harrison, 1992). The minimum temperature for germination of maize is in the range of 8–10 °C (Lütke Entrup & Oehmichen, 2000, Hellmers & Warrington, 1982). At the agricultural test site Wagna the average soil temperature in 5 cm depth (which corresponds to the drilling depth of maize) at sowing is between 10 and 11 °C. Thus, the criterion for sowing maize adopted here is a minimum soil temperature of 11 °C in 5 cm depth. Soil temperature is derived from simulated air temperature by linear correlation for the months April and May. This is the period when soil temperature 5 cm beneath the surface exceeds 11 °C permanently (correlation is based on observed soil and air temperatures from 2004 to 2011 at Wagna test site). Thermal limits to crop development can be defined by a minimum thermal accumulation above a base temperature referred to as the thermal time (Monteith, 1981) or effective temperature sum *ETS* (Carter et al., 1991):

$$ETS = \sum (T_i - T_b) \text{ for } T_i > T_b$$

where T_i is the mean daily air temperature and T_b is the base temperature for the crop. Common base temperatures for maize range between 8 and 10 °C (Lütke Entrup & Oehmichen, 2000; Narciso et al., 1992; Doorenbos & Kassam, 1979; Shaw, 1977). In this research Tb = 8 °C is used, which corresponds to the model settings of SIMWASER/STOTRASIM and means that simulated maize growth is only possible if air temperature exceeds 8 °C. This also implicates that air temperature is one factor indicating the end of the vegetation period in autumn. Furthermore, the growth of maize is also limited by maturity, which depends on the phenology of the cultivated sort. Early sorts require a lower ETS for reaching maturity than late ones. In contrast, later sorts have a longer vegetative period, more time for organic material development and thus potentially higher yields. Excessively late sorts will not reach maturity, may have lower yields than earlier sorts and need to be dried artificially (causing additional cost). In the present work the end of the potential vegetation period is determined for every single year between 1961 and 2100 and for each of the four climate change scenarios. This is achieved by means of simulations with SIMWASER/STOTRASIM and considering all growth restricting factors.

3 Results

The results are generally presented as means for 30-year periods:

- Observation period: 1981–2010
- Short-term prediction period: 2011–2040
- Medium-term prediction period: 2041–2070
- Long-term prediction period: 2071–2100

3.1 Vegetation Period

Figure 7 shows the durations of the potential vegetation period and effective temperature sums ETS for the 30-year periods between 1981 and 2100 as averages of the four climate change scenarios. Figure 7a represents cultivation strategy 1 (see section 2.4), where due to a fixed date for harvesting at October 4th, the vegetation period of grain maize can only be enlarged in spring. The average vegetation period is seen to increase from 160 days in the observation period to 167 days in the long-term prediction period, while ETS rises from 1534 °C to 2078 °C. The potential vegetation periods for cultivation strategies 2 and 3 are identical and presented in Figure 7b. They are not limited by a fixed date in fall and the end of possible crop growth is determined by SIMWASER/STOTRASIM. As a result, the potential vegetation period from 1981 to 2010 is 26 days longer compared to CS1 in Figure 7a and increases up to 207 days in the long-term prediction period. This also causes a generally larger ETS of 1611 °C in the observation period and of 2245 °C in the long-term prediction period.

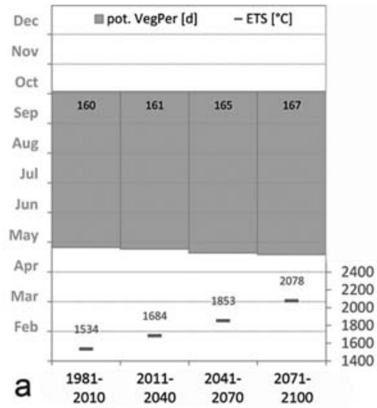

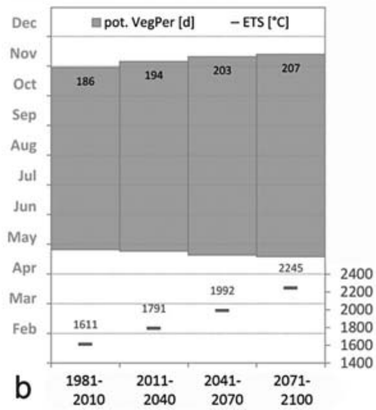

Figure 7: Potential vegetation periods and effective temperature sums ETS for (a) cultivation strategy 1 and (b) cultivation strategies 2 and 3

Abbildung 7: Potenzielle Vegetationsperiode (pot. VegPer) und effektive Temperatursummen (ETS) für (a) Kultivierungsvariante 1 und (b) Kultivierungsvarianten 2 und 3

3.2 Seepage Water

Model outputs for seepage water are presented in Figures 8a-1 (*CS1*), 8a-2 (*CS2*) and 8a-3 (*CS3*). Results based on observed weather data during the observation period range between 325 and 332 mm/a for the three cultivation strategies. The characteristics of the various climate change scenarios for all three cultivation strategies are similar. Groundwater recharges in the short-term period slightly decrease on average, which is followed by an increase of approximately 70 mm/a in the medium-term period. In the long-term period average predicted seepage rates are 375 and 391 mm/a for *CC1* and *CC2*/*CC3*, respectively. Maximum differences between the four climate change scenarios occur in the medium-term period and are approximately 200 mm/a.

3.3 NO_3 Concentration in Seepage Water

The nitrate concentration in the seepage water is characterized by an increasing trend (Figures 8b-1, 8b-2 and 8b-3). The differences between the observation period and the long-term prediction period are 11 and 13 mg/L for *CS1* and *CS3*, respectively. The most significant increase occurs between the observation and short-term prediction period in *CS3* with 9 mg/L.

3.4 NO_3-N Leaching

Nitrogen leaching is given in Figures 8c-1 (*CS1*), 8c-2 (*CS2*) and 8c-3 (*CS3*). A generally increasing trend of leached nitrogen for all cultivation scenarios is evident. While *CS1* and *CS2* start at about 27 kg N/ha/a in the observation period, the corresponding value for *CS3* is 44 kg N/ha/a. The overall average N leaching rates over the entire period from 1981 to 2100 are found to be 33 kg N/ha/a for *CS1*, 39 kg N/ha/a for *CS2* and 58 kg N/ha/a for *CS3*.

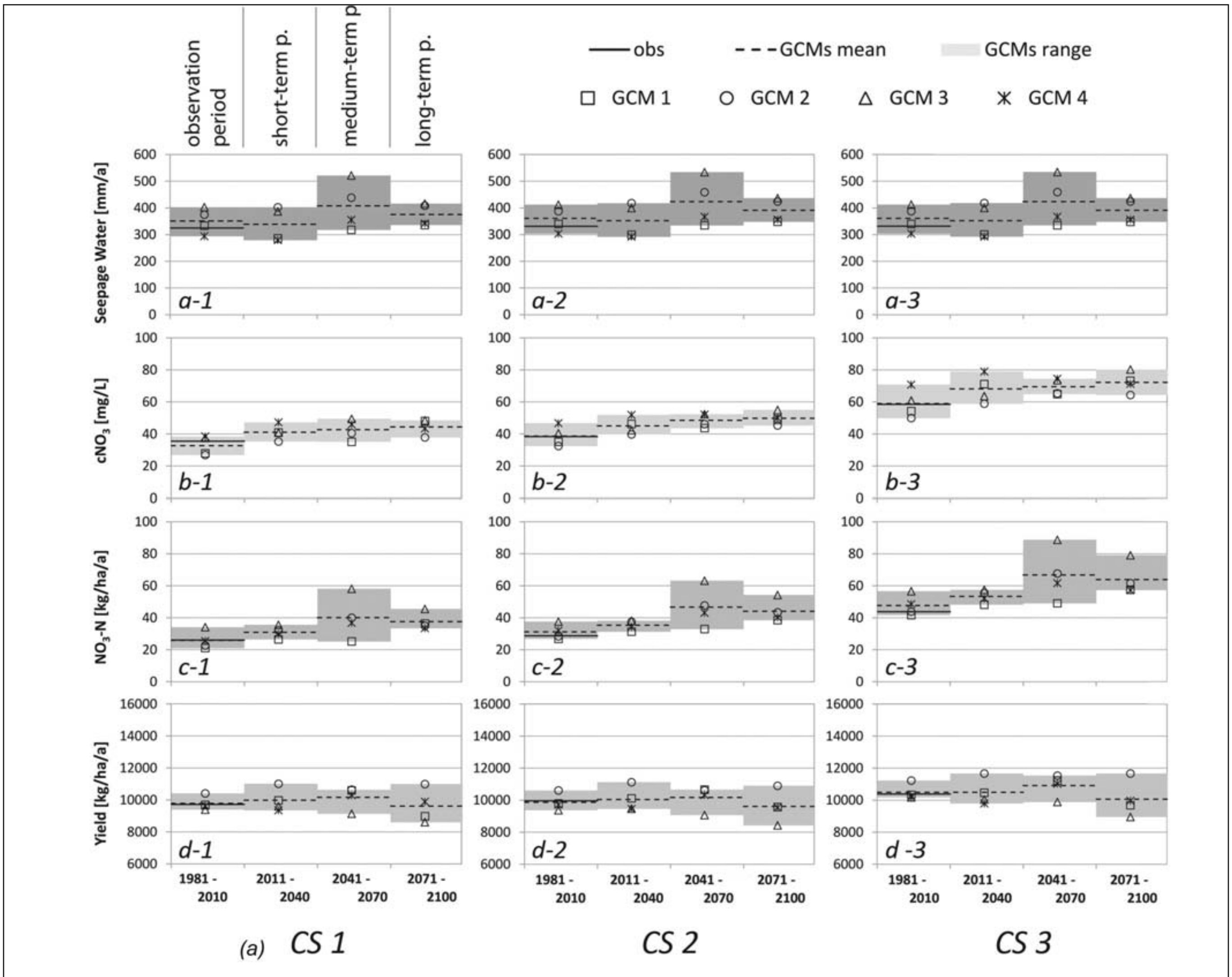

Figure 8: (a) Simulated seepage water, (b) nitrate concentrations in the seepage water, (c) nitrogen leaching and (d) maize yields for cultivation strategies 1, 2 and 3 using observed weather data (obs) and four climate change scenarios (GCMs 1–4) valid for the soil profile given in section 2.3 from 1981 to 2100 averaged over 30-year periods

Abbildung 8: Simulationsergebnisse für (a) Sickerwasser, (b) Nitratkonzentrationen im Sickerwasser, (c) Stickstoffauswaschung und (d) Maiserträge für Kultivierungsvarianten 1, 2 und 3 unter Verwendung von gemessenen Wetterdaten (obs) sowie der vier Klimawandelszenarien (GCMs 1–4) gültig für das in Kapitel 2.3 präsentierte Bodenprofil für den Zeitraum 1981–2100 (gemittelt über 30-jährige Perioden)

3.5 Maize Yields

Yield prediction for grain maize based on the four climate change scenarios does not indicate a big change in average yields at short and medium term, but show a larger spread compared to the observation period (Figures 8d-1, 8d-2 and 8d-3). Highest yields are simulated in the medium-term, followed by a sharp drop in yields in the long-term period. In the observation period maize yields for *CS1*, *CS2* and *CS3* are 9.700, 9.950 and 10.350 kg/ha/a, respectively.

4 Discussion

Although rising temperatures increase the grass reference evapotranspiration (ALLEN et al., 1998), the real evapotranspiration for maize is predicted to remain at a constant level (Tab. 2). This can be attributed to the limited water availability. Thus, future seepage water development based on the climate change scenarios considered is mainly driven by future precipitation patterns. Figure 9 shows the precipitation averaged for the prediction periods. It is obvious that the general trends in precipitation is of the same type as the predicted behavior of seepage water shown in Figures 8a-1, 8a-2 and 8a-3. E.g., the precipitation increase between the short and medium-term prediction periods of 78 mm/a corresponds well to the average increase in seepage water flow of 70 mm/a (*CS1*, *CS2* and *CS3*). Comparing the absolute values of seepage there is a slight difference between *CS1* and *CS2*/*CS3* due to a different vegetation period and the missing hardy catch crop in *CS3*. Different applied N fertilization rates do not influence seepage water flow significantly, which is reflected by equal results for *CS2* (140 kg N/ha/a) and *CS3* (200 kg N/ha/a).

Table 2: Grass reference evapotranspiration ET_0 and real evapotranspiration ETr of cultivation strategies 1, 2 and 3 for the observation and the prediction periods
Tabelle 2: Grasreferenz-Evapotranspiration ET_0 und reale Evapotranspiration ETr von Kultivierungsvariante 1, 2 und 3 für die Beobachtungs- und Prognoseperioden

Period	ET_0	ET_r (CS1)	ET_r (CS2)	ET_r (CS3)
		[mm]		
1981-2010:	708	583	574	573
2011-2040:	716	581	567	567
2041-2070:	718	589	574	574
2071-2100:	746	578	562	562

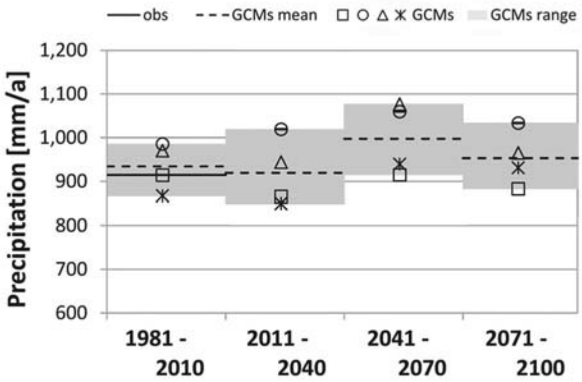

Figure 9: Observed (obs) and simulated (GCMs) total annual precipitation for Wagna, Austria, from 1981 to 2100 averaged over 30-year periods
Abbildung 9: Gemessener (obs) und simulierter (GCMs) Jahresniederschlag für Wagna, Österreich, von 1981 bis 2100 (gemittelt über 30-jährige Perioden)

NO_3-N leached into the groundwater is strongly correlated to seepage water flow. That is, the higher the seepage water flow, the higher is the NO_3-N leaching. Furthermore, and in contrast to results of seepage water, the general level of NO_3-N leaching depends on N fertilization rates. E.g., an increase of the N fertilization rate from 140 to 200 kg/ha/a between *CS2* and *CS3* results in an increase of approximately 20 kg/ha/a NO_3-N leaching on average over the entire modeling period. Moreover, NO_3-N leaching also depends on whether or not a hardy catch crop is cultivated. The effect of the hardy catch crop can be seen by comparing *CS1* with *CS2* (Figures 8c-1 and 8c-2). Even though the vegetation period of the main crop in *CS2* is larger than in *CS1*, the NO_3-N leaching rises without a hardy catch crop.

The influence of hardy catch crops and the N fertilization rate is also visible for results of nitrate concentrations. E.g., looking at the observation period in Figures 8b-1, 8b-2 and 8b-3, the difference of nitrate concentration for simulations using observed weather data is 10 % between *CS1* and *CS2*. This can be explained by the missing hardy catch crop. Between *CS2* and *CS3* there is a difference of 50 % due to a 60 kg/ha/a higher N fertilization rate. Furthermore, the combination of a missing hardy catch crop and a higher N fertilization rate results in a 60 % higher nitrate concentration in the seepage water between *CS1* and *CS3*. In general, while the nitrate concentrations in the seepage water of all cultivation scenarios start from different concentration levels, their predicted future behaviors follow the same increasing trend.

Temperature is an important driving force for plant growth and crop production. However, even for rising effective temperature sums *ETS*, crop yields presented in Figures 8d-1, 8d-2 and 8d-3 do not show a significant increase and decreasing crop yields are simulated in the long-term period. This fact can be attributed to an insufficient water supply. I.e., crop water requirements cannot be covered by rain for the investigated location in Wagna at all times, drought stress occurs and crop growth is restricted. This statement is verified in a further model run where *CS1* is simulated with optimal water supply for maize (irrigation if matrix potential lower –700 hPa in 40 cm depth). It can be seen in Figure 10 that the combination of temperature increase without drought stress results in generally higher crop yields of maize (due to optimal water supply of the plant) and that maize yields further increase in the future (due to the temperature increase). It may be observed that the calculated crop yields using the observed weather data is beyond the range of the climate change scenarios in the observation period. However, the level of yield between 13.000 kg/ha/a (mean of GCMs) and 14.000 kg/ha/a (observed weather data) appears plausible compared to measured crop yields for the location "Wagendorfer Terrasse", where profound clayey soils with high water storage capacity and only little drought stress conditions are present (VERSUCHSREFERAT STEIERMARK, 2012).

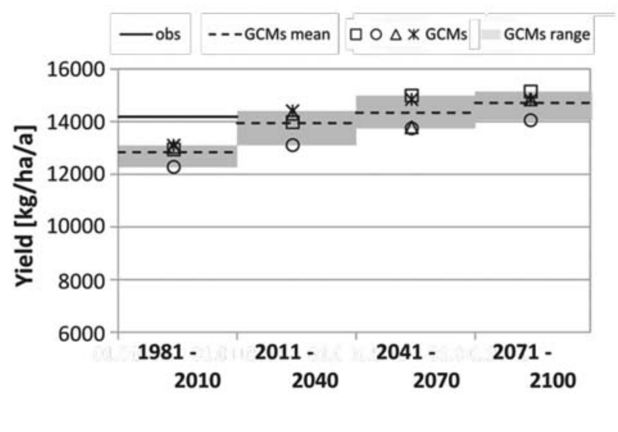

Figure 10: Simulated maize yields for CS1 assuming optimal crop water supply in combination with observed weather data (obs) and four climate change scenarios (GCMs) valid for the soil profile given in section 2.3 from 1981 to 2100 averaged over 30-year periods

Abbildung 10: Simulierte Maiserträge für Kultivierungsvariante 1 unter Annahme von optimaler Wasserversorgung der Pflanze bei Verwendung von gemessenen Wetterdaten (obs) und vier Klimawandelszenarien (GCMs 1–4) gültig für das in Kapitel 2.3 präsentierte Bodenprofil für den Zeitraum 1981–2100 (gemittelt über 30-jährige Perioden)

Focusing on crop yields for the observation period determined by means of observed weather data between 1981 and 2010 (solid line in Figures 8d-1, 8d-2 and 8d-3) it can be seen that differences are +250 kg/ha/a between *CS1* and *CS2* and +650 kg/ha/a between *CS1* and *CS3*. In addition, the respective increases in nitrate concentrations in the seepage water are 10 % and 60 % for *CS2* and *CS3* compared to *CS1*. This indicates that a rather low yield increase of approx. 7 % between CS1 and CS3 may cause a significant worsening of the seepage water quality for the investigated location. This highlights the importance of applying adequate N fertilization rates.

5 Conclusions

The significance of the ensemble modeling approach is underlined by the rather large variability in results for seepage water and nitrate flux between the four climate change scenarios. Considering the average results out of these four scenarios, there is an increasing trend of groundwater recharge, nitrogen leaching and nitrate concentration in the seepage water in general. For the investigated location, this implies that there will be no natural improvement of the groundwater nitrate concentration due to likely weather conditions in the future.

Although there is a predicted temperature increase of approximately 3 °C until the year 2100 and with it an enlargement of the potential vegetation period, crop yields for maize are not predicted to increase significantly. Future maize yields for the location of Wagna, Austria, will only increase if drought stress is avoided (e.g. by irrigation). Thus, our conclusion is along the lines of KANG et al. (2009) that crop yields are more sensitive to precipitation than to temperature. The combination of sufficient water supply of plants and higher temperatures would increase maize yields considerably.

The differences in maize yields using the observed weather data in combination with the three cultivation strategies are rather low. In contrast, respective nitrate concentrations in the seepage water of *CS3* are significantly higher than those for *CS1* and *CS2*. Hence, future work will focus on an assessment of the entire economic balance of agricultural holdings (e.g., costs for fertilizer, transport, etc.) in order to investigate whether or not cultivation strategies using high nitrogen fertilization rates are in fact more economic than groundwater protecting cultivation strategies. Although the present results are based on a model calibration to data from the Wagna test site, they can be assumed to be representative for most parts of the Murtal aquifer. Future work may encompass a regional simulation of groundwater recharge, nitrogen leaching and crop yields based on climate change scenarios and including a sequential coupling with a groundwater flow and transport model. Doing so, the additional influence of different soil conditions and cultivated crops may be evaluated.

Acknowledgement

The work was carried out as part of the GENESIS project on groundwater systems (http:/www.thegenesisproject.eu) financed by the European Commission 7FP contract 226536.

References

AG BODEN (Ad-hoc-Arbeitsgruppe Boden) (2005): Bodenkundliche Kartieranleitung. Bundesanstalt für Geowissenschaften und Rohstoffe in Zusammenarbeit mit den Staatlichen Geologischen Diensten (Ed.), 5. Aufl., Hannover.

ALLEN, R.G., L.S. PEREIRA, D. RAES & M. SMITH (1998): Crop Evapotranspiration – Guidelines for Computing Crop Water Requirements. FAO Irrigation and Drainage Paper 56. United Nations FAO, Rome, Italy.

BMLFUW (Bundesministerium für Land- und Forstwirtschaft, Umwelt und Wasserwirtschaft) (2006): Richtlinien für die sachgerechte Düngung. Anleitung zur Interpretation von Bodenuntersuchungsergebnissen in der Landwirtschaft. 6. Aufl., Bundesministerium für Land- und Forstwirtschaft, Umwelt und Wasserwirtschaft, Wien.

CARTER, T.R., M.L. PARRY & J.H. PORTER (1991): Climatic change and future agroclimatic potential in Europe. Int. J. Climatol. 11: 251–269.

CUCULEANU, V., P. TUINEA & D. BĂLTEANU (2002): Climate change impacts in Romania: vulnerability and adaptation options. GeoJournal, 57(3): 203–209.

DOORENBOS, J. & A.H. KASSAM (1979): Yield response to water. FAO irrigation and drainage paper 33. Food and Agricultural Organization of the United Nations, Rome.

ECKHARDT, K. & U. ULBRICH (2003): Potential impacts of climate change on groundwater recharge and streamflow in a central European low mountain range. J. Hydrol., 284 (1–4): 244–252.

FADER, M., S. ROST, C. MÜLLER, A. BONDEAU & D. GERTEN (2010): Virtual water content of temperate cereals and maize: Present and potential future patterns. J. Hydrol. 384 (1–4): 218–231, doi:10.1016/j.jhydrol.2009.12.011.

FEICHTINGER, F. (1998): STOTRASIM – Ein Modell zur Simulation der Stickstoffdynamik in der ungesättigten Zone eines Ackerstandortes. In: Modelle für die gesättigte und ungesättigte Bodenzone. Schriftenreihe des Bundesamtes für Wasserwirtschaft, Wien, 7: 14–41.

GODERNIAUX, P., S. BROUYÈRE, H.J. FOWLER, S. BLENKINSOP, R. THERRIEN, P. ORBAN & A. DASSARGUES (2009): Large scale surface-subsurface hydrological model to assess climate change impacts on groundwater reserves. J. Hydrol. 373 (1–2), 122–138.

GORDON, C., C. COOPER, C.A. SENIOR, H. BANKS, J.M. GREGORY, T.C. JOHNS, J.F.B. MITCHELL & R.A. WOOD (2000): The simulation of SST, sea ice extents and ocean heat transports in a version of the Hadley Centre coupled model without flux adjustments, Climate Dynamics, 16: 147–168, doi:10.1007/s003820050010.

GRAUX, A.I., G. BELLOCCHI, R. LARDY & J.F. SOUSSANA (2012): Ensemble modeling of climate change risks and opportunities for managed grasslands in France. Agr. Forest Meteorol., accepted, http://dx.doi.org/10.1016/j.agrformet.2012.06.010.

GWD (2006): Directive 2006/118/EC of the European Parliament and of the Council of 12 December 2006 on the protection of groundwater against pollution and deterioration. Official Journal of the European Union, http://eur-lex.europa.eu/LexUriServ/LexUriServ.do?uri=OJ:L:2006:372:0019:0031:EN:PDF (valid on December 17th, 2012).

HELLMERS, H. & I. WARRINGTON (1982): Temperature and plant productivity. In: Rechcigl, M. (Ed.) CRC handbook of agricultural productivity, Vol. 1 CRC, Boca Raton, 11–21.

IPCC (2007): Climate Change 2007: The Physical Science Basis. Contribution of Working Group I to the Fourth Assessment Report of the Intergovernmental Panel on Climate Change. SOLOMON, S., D. QIN, M. MANNING, Z. CHEN, M. MARQUIS, K.B. AVERYT, M. TIGNOR & H.L. MILLER (Ed.) Cambridge University Press, Cambridge, UK.

JACKSON, C.R., R. MEISTER & C. PRUDHOMME (2011): Modelling the effects of climate change and its uncertainty on UK Chalk groundwater resources from an ensemble of global climate model projections. J. Hydrol., 399(1–2): 12-28, doi:10.1016/j.jhydrol.2010.12.028.

KANG, Y., S. KHAN & M. XIAOYI (2009): Climate change impacts on crop yield, crop water productivity and food security – A review. Prog. Nat. Sci., 19(12): 1665–1674, doi:10.1016/j.pnsc.2009.08.001.

KENNY, G.J. & P.A. HARRISON (1992): Thermal and moisture limits of grain maize in Europe: model testing and sensitivity to climate change. Clim. Res., 2: 113–129.

KJELLSTRÖM, E., G. NIKULIN, U. HANSSON, G. STRANDBERG & A. ULLERSTIG (2011): 21st century changes in the European climate: uncertainties derived from an ensemble of regional climate model simulations. Tellus A, 63: 24–40, doi: 10.1111/j.1600-0870.2010.00475.x.

KLAMMLER, G., H. KUPFERSBERGER, G. ROCK & J. FANK (2013): Modeling coupled unsaturated and saturated nitrate distribution of the aquifer Westliches Leibnitzer Feld, Austria. – Environ. Earth Sci., doi:10.1007/s12665-013-2302-6.

LÜTKE ENTRUP, N. & J. OEHMICHEN (Eds.) (2000): Lehrbuch des Pflanzenbaues – Band 2: Kulturpflanzen. Verlag Th. Mann, Gelsenkirchen.

MERRITT, W.S., Y. ALILA, M. BARTON, B. TAYLOR, S. COHEN & D. NEILSEN (2006): Hydrologic response to scenarios of climate change in sub watersheds of the Okanagan basin, British Columbia. J. Hydrol. 326(1–4): 79-108, doi:10.1016/j.jhydrol.2005.10.025.

MONTEITH, J.L. (1981): Climatic variation and the growth of climate change: the IPCC impacts assessment. Australian Government Publishing Service, Canberra, 3-1-3-43.

NAKIĆENOVIĆ, N. & R. SWART (Eds.) (2000): Special report on emissions scenarios. In: A Special Report of Working Group III of the Intergovernmental Panel on Climate Change. Cambridge University Press, Cambridge, UK.

NARCISO, G., P. RAGNI & A. VENTURI (1992): Agrometeorological aspects of crops in Italy, Spain and Greece: a summary review of durum wheat, barley, maize, rice, sugar beet, sunflower, soybean, rape, potato, tobacco, cotton, olive and grape. Publication EUR 14124 EN of the Office for Official Publications of the European Communities; Series "Agriculture", Luxembourg.

NEUMEISTER, H. (Ed.) (2010): Oberflächennahe Erdsysteme. Leben-Wasser-Luft-feste Erde, systemisch raumzeitlich verbunden in 3D-Körpern, Transformations- und Funktionsräumen. Projekte Verlag Halle, 40.

ROECKNER, E., R. BROKOPF, M. ESCH, M. GIORGETTA, S. HAGEMANN, L. KORNBLUEH, E. MANZINI, U. SCHLESE & U. SCHULZWEIDA (2006): Sensitivity of simulated climate to horizontal and vertical resolution in the ECHAM5 atmosphere model. J. Clim., 19: 3771–3791.

SALAS-MÉLIA, D., F. CHAUVIN, M. DÉQUÉ, H. DOUVILLE, J.F. GUEREMY, F. CHAUVIN, S. PLANTON, J.F. ROYER & S. TYTECA (2005): Description and validation of the CNRM-CM3 global coupled model, CNRM Tech. Rep. 103.

SAMUELSSON, P., C.G. JONES, U. WILLÉN, A. ULLERSTIG, S. GOLLVIK, U. HANSSON, C. JANSSON, E. KJELLSTRÖM, G. NIKULIN & K. WYSER (2011): The Rossby Centre Regional Climate Model RCA3: model description and performance. Tellus A, 63: 4–23, doi: 10.1111/j.1600-0870.2010.00478.x.

SERRAT-CAPDEVILA, A., J.B. VALDES, J.G. PEREZ, K. BAIRD, L.J. MATA & T. MADDOCK (2007): Modeling climate change impacts and uncertainty on the hydrology of a riparian system: the San Pedro Basin (Arizona/Sonora). J. Hydrol., 347(1–2): 48–66.

SGV (2005): Verordnung des Landeshauptmannes von Steiermark vom 21. November 1990, mit der ein Grundwasserschongebiet zum Schutz der Wasserversorgungsanlagen der Leibnitzerfeld Wasserversorgung GmbH., der Marktgemeinde Lebring St. Margrethen und der Gemeinde Retznei bestimmt wird. Stammfassung: LGBl. Nr. 86/1990, Novelle: LGBl. Nr. 48/2006, Graz, Austria.

SHAW, R.H. (1977): Climatic requirement. In: SPRAGUE, G. F. (Ed.) Corn and corn improvement. American Society of Agronomy, Madison, Wisconsin, 591–623.

STENITZER, E. (1988): SIMWASER – Ein numerisches Modell zur Simulation des Bodenwasserhaushaltes und des Pflanzenertrages eines Standortes. Mitt. der Bundesanstalt für Kulturtechnik und Bodenwasserhaushalt, 31: 1–118, Petzenkirchen.

SURFLEET, C.G., D. TULLOS, H. CHANG & I.W. JUNG (2012): Selection of hydrological modeling approaches for climate change assessment: A comparison of model scale and structures. J. Hydrol., 464–465: 233–248, http://dx.doi.org/10.1016/j.jhydrol.2012.07.012.

SZEICZ, G., G. ENDRÖDI & S. TAJCHMAN (1969): Aerodynamic and surface factors in evaporation, Water Resour. Res., 5(2): 380–394, doi:10.1029/WR005i002p00380.

THOM, A.S. & H.R. OLIVER (1977): On Penman's equation for estimating regional evaporation. Q.J.R. Meteorol. Soc., 103: 345–357, doi:10.1002/qj.49710343610.

VERSUCHSREFERAT STEIERMARK (2012): Versuchsbericht 2011. Amt der Steiermärkischen Landesregierung, Fachabteilung 6C, Land-und forstwirtschaftliches Berufs- und Fachschulwesen, Referat Versuchstätigkeit.

Voldoire, A., E. Sanchez-Gomez, D. Salas y Mélia, B. Decharme, C. Cassou, S. Sénési, S. Valcke, I. Beau, A. Alias, M. Chevallier, M. Déqué, J. Deshayes, H. Douville, E. Fernandez, G. Madec, E. Maisonnave, M.P. Moine, S. Planton, D. Saint-Martin, S. Szopa, S. Tyteca, R. Alkama, s. Belamari, A. Braun, L. Coquart & F. Chauvin (2011): The CNRM-CM 5.1 global climate model: description and basic evaluation, Clim. Dyn., doi:10.1007/s00382-011-1259-y.

Woldeamlak, S.T., O. Batelaan & F. De Smedt (2007): Effects of climate change on the groundwater system in the Grote-Nete catchment, Belgium. Hydrogeol. J., 15(5), 891–901.

Yang, W., A. Bárdossy & H.J. Caspary (2010a): Downscaling daily precipitation time series using a combined circulation- and regression-based approach. Theor. Appl. Climatol., 102: 439–454, doi:10.1007/s00704-010-0272-0.

Yang, W., J. Andreásson, L.P. Graham, J. Olsson, J. Rosberg & L. Wetterhall (2010b): Distribution-based scaling to improve usability of regional climate model projections for hydrological climate change impacts studies. Hydrol. Res., 41(3–4): 211–228.

Address of authors

Mag. Gernot Klammler, Univ.-Doz. Dr. Johann Fank, Univ.-Doz. DI Dr. Hans Kupfersberger, Joanneum Research Graz, Resources – Institute for Water, Energy and Sustainability, Elisabethstraße 18/II, 8010 Graz

Submitted: January 4, 2013
Accepted: June 13, 2013